

APPLICATION OF THE MOVING-SLIT X-RAY AUTOMONOCROMATIZATION METHOD IN STRUCTURAL STUDIES OF PLANAR DIODES AND AN ATTEMPT TO CORRELATE ELECTRICAL PROPERTIES WITH LATTICE DEFECTS

BY J. AULEYTNER, Z. FURMANIK AND J. KRYŁOW*

Institute of Physics, Polish Academy of Sciences**

(Received May 29, 1971; Revised paper received November 29, 1971)

The X-ray automonochromatization method and the Lang method are applied in the detection of structural defects in silicon slices with planar diodes. An attempt was made to establish a qualitative correlation between defects in the crystal region limited by the window in the SiO₂ and the electrical properties of the diodes. It was found that certain types of defects bear a strong effect on diode electrical properties. The adequacy of the X-ray automonochromatization method for quick determinations of the defect structure in silicon slices is demonstrated.

Planar diodes and transistors are the basic elements of modern electronic devices. The process by which each of these elements is manufactured is long and rather complicated. In the case of single diodes or transistors it consists in properly preparing oriented single-crystalline slices of *n*- or *p*-type silicon, depositing an *n*- or *p*-type epitaxial layer, thermal oxidation, producing appropriate windows by a photolithographic technique, diffusing or implanting impurities, making contacts, heating the product and performing the final encapsulation. During these steps many new defects may form, and they bear an immense effect on the physical and technical properties of the elements being produced. From this point of view, therefore, immediate control of technological processes would have enormous significance, for both practice and science because it would enable to relate better the physical properties of the materials with their defect structure¹.

* Address: Instytut Technologii Elektronowej, Warszawa, Świętokrzyska 21, Poland.

** Address: Instytut Fizyki PAN, Warszawa, Zielna 37, Poland.

¹ Already now there is work being carried out in some centres of highly-developed countries on the determination of the conditions under which defects form in semiconducting elements at each manufacturing stage and their effect on the electrical properties of the finished product (Whelan 1969, Serebrinsky 1970, Schwuttke 1970, Gri 1971). This type of research is essential and in many cases permit changes in technology eliminating the formation of defects to be introduced. The development of such research stems from the ever increasing degree of integration of semiconducting circuits, in which defects are a factor considerably affecting the gain of good devices.

Recent years have seen the development of many non-destructive methods of detecting defects. These are rarely applied in industry, however, because technology requires fast acquisition of information in order to be able to properly and efficiently control technological processes. Unfortunately, the methods in mention are very time-consuming, and it is therefore very important for the development of electronics to improve measuring techniques so they could effectively be applied in the control of the manufactured elements at the various stages of production. The technique employing an X-ray spectrograph with an oscillating slit (Auleytner 1971) allows defects in thin single crystals to be detected much faster than, *e. g.*, by Lang's technique (Lang 1958).

This paper presents an attempt of applying this technique to defect detection in planar diodes and linking their electrical properties with the defects. X-ray topograms were obtained both in transmission and in reflection. The edges of the windows etched in the SiO₂ layer show up in the X-ray image as darkened lines. Extinction contrast appears here because there are strains in the single-crystalline silicon slices due to interaction of the silicon oxide layer. The immediate cause of the strains is the difference in coefficients of linear expansion. This contrast depends of the indices of the diffracting plane. As has been show (Howard and Schwuttke 1967, Schwuttke 1970), in the window-edge region the relative strain changes as $\cos \angle(g, R_i)$ as regards sign and magnitude, where g is the diffraction vector and R_i is a vector identifying the given edge (R_i is perpendicular to the edge i). The gradient of strains is perpendicular to the window edge, the position of which is characterized by the vector R_i (Fig. 1). The gradient of strains is colinear with vector R_i . The best contrast

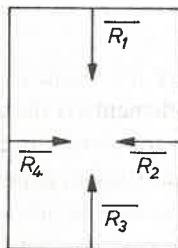


Fig. 1. Directions of vectors identifying window edges and characterizing the gradient of strains at the SiO₂-Si interface

is achieved when $\angle(g, R_i) = 0$, thus $\cos \angle(g, R_i) = 1$ (Howard and Schwuttke 1967). This contrast makes it possible to image by a photographic technique the window regions whereby the impurities are introduced. When resolving power is high, this method may also reveal lattice defects in the window region, such as dislocations, and this enables their effect on the characteristics of the diode to be examined.

In our case a 5000 Å thick layer of SiO₂ was thermally overgrown on *n*-type silicon slices of resistivity 2.2 Ω cm. Next, a layer of aluminum 0.5 μm thick was deposited on the SiO₂. Square windows of a side of 0.6 mm were etched in both layers. The slices prepared thus then had gallium ions implanted in them; the energies in succession were: 40 keV - 1.8 × 10¹⁴ ions/cm²; 30 keV - 1.8 × 10¹⁴ ions/cm²; 20 keV - 1.7 × 10¹⁴ ions/cm²; and 10 keV - 1.7 × 10¹⁴ ions/cm². This gives a total of 7 × 10¹⁴ ions/cm². The Al layer on the

SiO_2 restricted implantation to the window region and safeguarded the SiO_2 against radiation damages. After accomplishment of implantation the Al layer was removed, and the slice was cut into strips which were then heated to 500°C (360 B/1sample) and 800°C (360 B/4 sample) for 30 minutes in an atmosphere of argon. The heating had the purpose of removing any radiation defects in the implanted layer. Ohmic contact with the sample substrate was achieved by electroless plating of nickel with a phosphorus addition (heating at 460°C for 10 min). Aluminum contacts were deposited onto the window region by evaporation at 200°C . Before applying the aluminum, the surface layers of oxide were removed off the window regions by rinsing the samples in diluted hydrofluoric acid.

The thin implanted layers, of the order of several hundred Å's, made it impossible to deposit contacts at higher temperatures because of the possibility of Al diffusion. The ohmic behaviour of the contacts obtained thus was not checked, and these contacts may rectify current, what would complicate the electrical effects of the junctions between the substrate and implanted layer. The accomplishment of ohmic contacts to implanted layers is a difficult problem to solve and will be the topic of future papers.

The setup for measuring the voltage-current characteristics gave an accuracy between 10 and 20 per cent. The voltage-capacitance characteristics were measured at a frequency of one MHz with an accuracy of several per cent.

Defects were detected by means of the method of *X*-ray automonochromatization by an oscillating slit (Auleytner 1971). The slices were approximately 0.3 mm thick. When the topography of the interior was sought, the characteristic K_α radiation of molybdenum was used, whereas that of the surface was obtained with the use of the characteristic K_α radiation of copper. Figure 2 presents the *X*-ray diffraction pattern of the interior of a silicon platelet coated with an SiO_2 layer. The various diode windows can be seen, as well as their structure (electrical characteristics of these diodes have been measured). The visible contrast at the two mutually perpendicular window edges (horizontally this is much weaker) is caused by the fact that to get the 220 reflection in this case required the platelet to be oriented on the goniometer head of the spectrometer in such a way that $\varphi(g, R_i)$ be about 30° . At the upper part of the figure we see a higher density of dislocations than at the bottom. Apart from this, inside some windows one may notice the presence of larger defects, hitherto unidentified, which cause quite strong deformation of the pattern. Such is the case, *e. g.*, for windows 8 and 9. These are not surface defects, for the topographs found by the reflection method (*e. g.*, Fig. 3) do not exhibit any deformation of these windows.

Further examination showed that it is precisely when defects of this type appear in a diode that the worst electrical characteristics are observed. The latter for these diodes are shown in Figs 8a and 8b.

Figures 4a and 4b concern another example of a slice with planar diodes. The topograms were obtained from the 220 and 422 reflections of the beam transmitted by the sample (*i. e.* the transmission case). We see that the diffraction pattern of the 220 type in this case reveals much fewer defects than the 422 pattern, which revealed a dense network of dislocations inside the slice. These dislocations, as was later found, bear a large effect on the electrical characteristics (Figs 9a, b, c, and Table I).

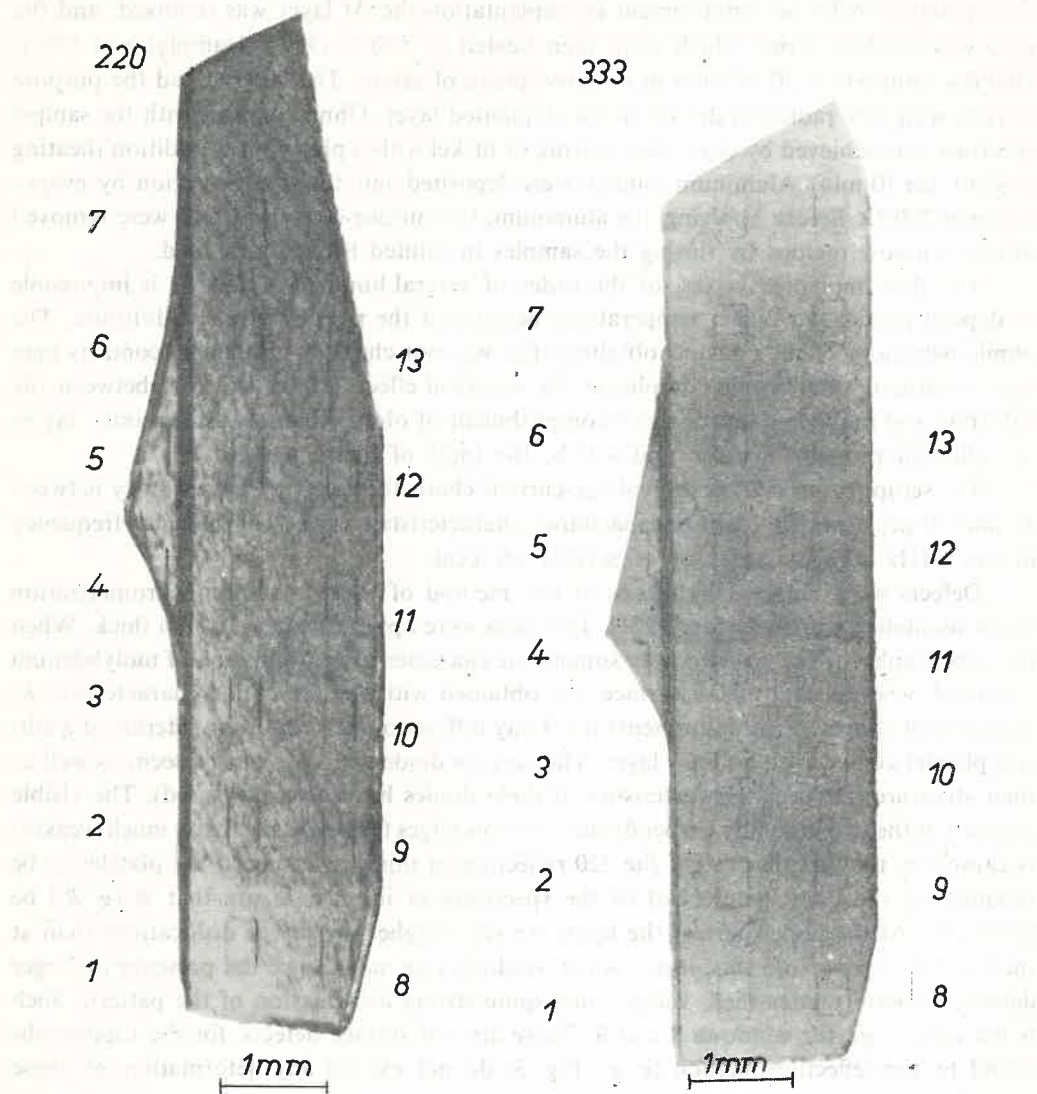


Fig. 2

Fig. 3

Fig. 2. X-ray diffraction pattern of interior of a single-crystalline silicon slice 360B/1 overgrown with an SiO_2 layer having etched windows implanted with gallium after heating at 500°C . The windows show up as darker contours thanks to diffraction contrast due to strains. Radiation: $K_2\text{Mo}$. Effective dimension of point focus approx. $30\ \mu\text{m}$. Voltage and current respectively: 45 kV and 360 μA . Plates: Ilford nuclear; emulsion thickness: $50\ \mu\text{m}$; exposure: 4 hrs; Reflection: 220. Slice thickness: approx. 0.3 mm

Fig. 3. X-ray diffraction pattern of the surface of the same single crystal as in Fig. 2. in reflection. Reflection: 333. Radiation: $K_2\text{Cu}$. Voltage and current respectively: 38 kV and 400 μA . Focus: $30\ \mu\text{m}$. Exposure: 3.5 hrs; plates: Gevert

Figures 5a and b show by way of illustration the X-ray pattern of the interior of planar diodes produced on a *n*-type silicon slice of resistivity $2.2 \Omega \text{ cm}$. This slice (356A/2) was prepared just like the 360B/1 and 360B/4 systems, except that instead of implanting galium ions use was made of boron ions of the successive energies: 40 keV — 1.83×10^{14} ions/cm²; 30 keV — 1.55×10^{14} ions/cm²; 20 keV — 1.73×10^{14} ions/cm²; and 10 keV — 0.27×10^{14}

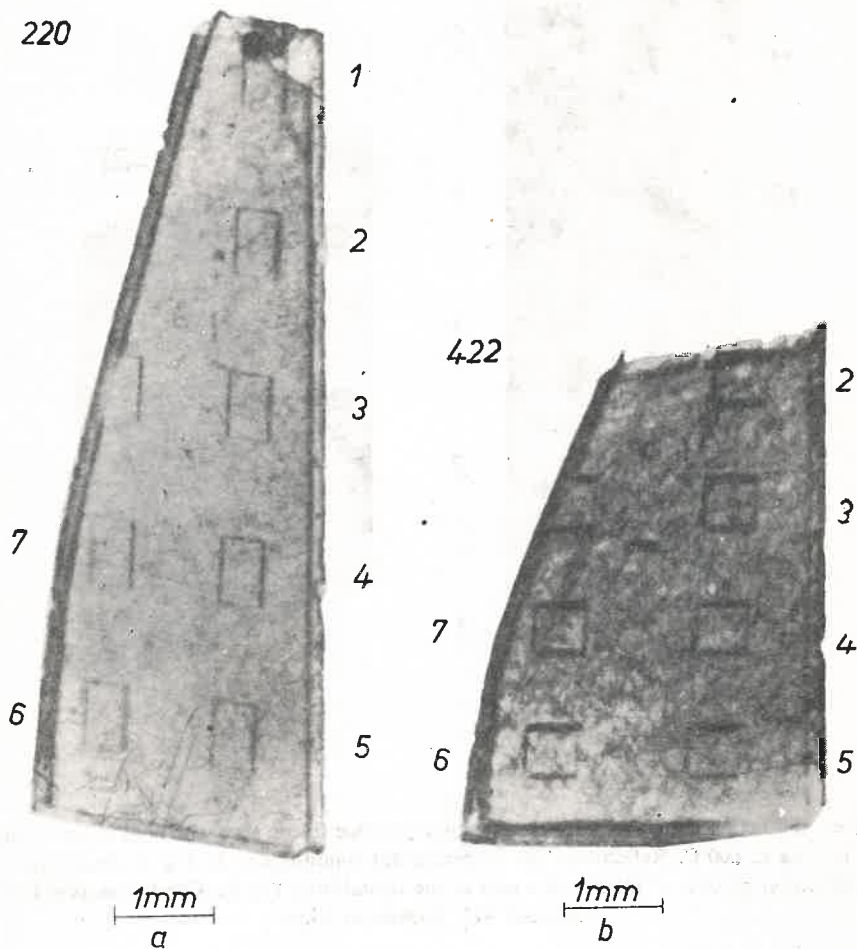


Fig. 4a. X-ray diffraction pattern of interior of single-crystalline silicon slice 360 B/4 covered with SiO_2 layer having etched windows implanted with galium after heating at 800°C . Reflection: 220. Radiation: K_2Mo . Voltage and current respectively: 48 kV and 380 μA . Exposure: 4 hrs. Plates: Ilford nuclear; emulsion thickness: 50 μm ; b. X-ray diffraction pattern of interior of the same crystal and in Fig. 4a. Reflection: 422. Exposure: 8 hrs. Experimental conditions the same as in Fig. 4a

ions/cm², giving a total of 5.38×10^{14} ions/cm². After implantation the sample was heated at 600°C in an argon atmosphere for 30 minutes. In this case the 422 reflection shows up such a dense network of defects surrounded by large disturbance fields that the window

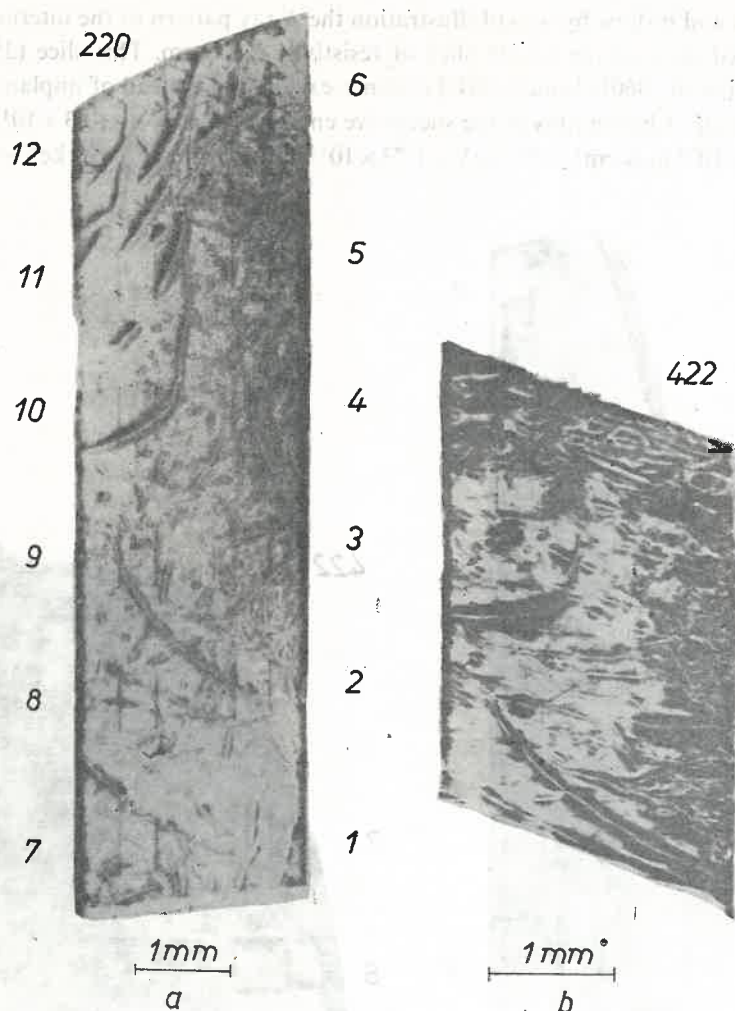


Fig. 5a. X-ray diffraction pattern of interior of single-crystalline silicon slice with high impurity concentration after heating at 600°C. Reflection: 220. Experimental conditions as in Fig. 2. Exposure: 3.75 hrs; b. X-ray diffraction pattern of interior of a part of the crystal from Fig. 5a. Conditions as in Fig. 5a. Reflection: 422. Exposure: 5 hrs

edges are almost obscured. We probably encounter here the phenomenon of dislocation decoration by the impurities present in the initial material.

Figures 6a and b show the diffraction patterns found for the same set of planar diodes by Lang's technique with the use of another 422 type reflection². This method permitted section topographs to be obtained. Figure 6a shows the transmission topogram of the whole crystal, whereas Fig. 6b only that of the layer B (*cf.* Fig. 6c). The topogram presented

² These photographs by K. Godwod.



Fig. 6a. X-ray diffraction pattern of interior of the same silicon slice as in Figs 5a and b obtained by Lang's method. Reflection type: 422. Experimental conditions as in Fig. 2. Exposure: 40 hrs; b. X-ray diffraction pattern of the B layer of the same silicon slice as in Fig. 6a, obtained by Lang's method. Reflection type: 422. Exposure: 38 hrs (cf. elucidating Fig. 6c)

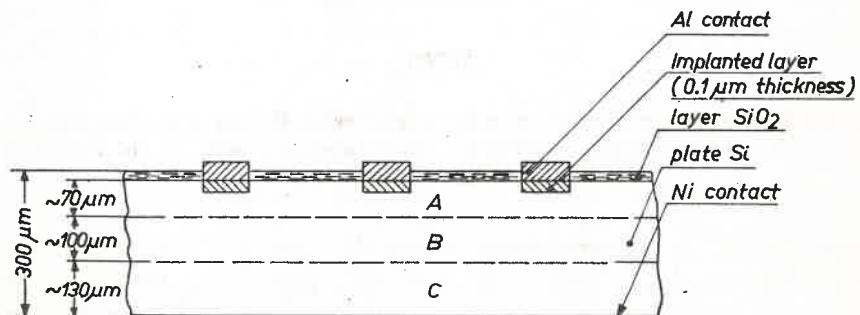


Fig. 6c. Cross-section of 356A/2 slice with planar diodes tentatively showing the crystal region imaged in Fig. 6b

in Fig. 7 was made by the method of the moving (oscillating) slit (Auleytner 1971) in reflection (333 reflection). Only a few defects are visible in it, what is proof that most of them are located inside the examined object. We note that both methods employed a PZPX-6 X-ray apparatus operating under identical conditions in both cases.

Recording of the interior image of the same object required from 3 to 4 hours in the case of the oscillating slit method and about 40 hours in the case of Lang's method. The sharpness of the obtained images is comparable.

The oscillating slit method may also be used when the single crystals to be examined are bent a little. Then, the divergence of the incident beam has to be increased somewhat

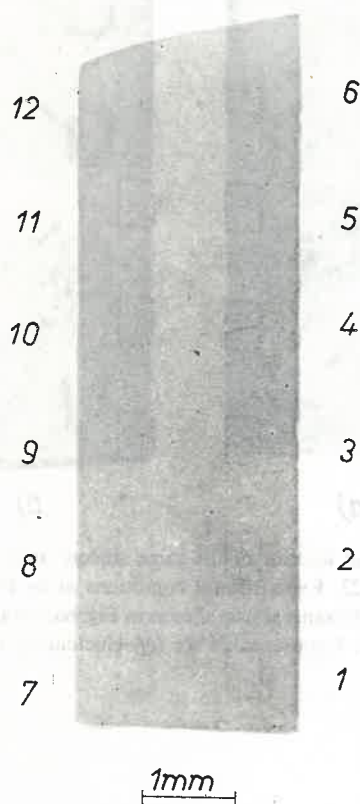


Fig. 7. X-ray diffraction pattern (in reflection) of the surface (region A) of the same silicon slice as in Figs 6a and b found by the method of the oscillating slit spectrometer. Exposure: 2.5 hrs. Radiation: K_{α} Cu. Reflection: 333

by widening the slit. At an appropriately chosen slit opening it is possible to reveal the distribution of strains at the surface of the examined crystal caused, for example, by poor technology of overgrowing the epitaxial layer. To improve resolving power K_{β} lines would have to be utilized in this case.

When attempting to establish the correlation between the X-ray image of defects in

the diode region and the diode's electrical characteristics we notice that in the case of the 360B/1 sample (Figs 2, 3 and 8a, b, c, d, e) there is strong perturbation of the structure in the region of windows 8 and 9 (Fig. 2) Moreover, the image suggests that the defects are dislocations steeply inclined with respect to the surface of the slice. These diodes have the largest leakages and the lowest breakdown voltages.

In the other windows the deformations due to defects are much smaller. The defects are arranged in a more uniform manner and do not introduce such pronounced deformations as in windows 8 and 9. Diode 1 lies in the region of a local bend in the crystal. It should be remembered that the correlation between the defect image and the electrical properties of planar diodes may be obscured by the considerable number of effects such as: surface leakage currents associated with recombination at the Si-SiO₂ interface, injection of the minority carriers by the contacts, the shape of interface between implanted and unimplanted area, and the large density of dislocations unevenly distributed, making an interpretation of the images of the various defect species visible in the diode windows rather difficult.

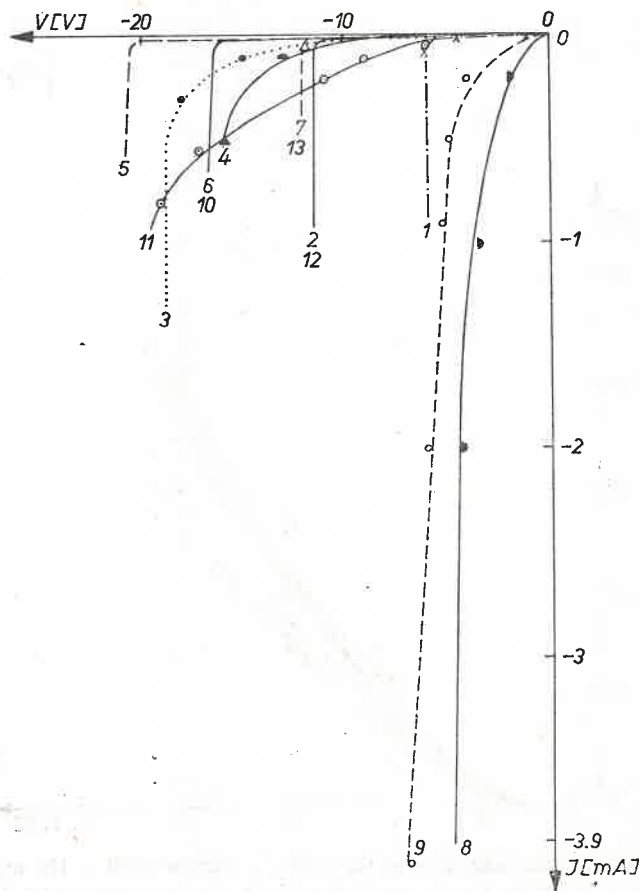


Fig. 8a

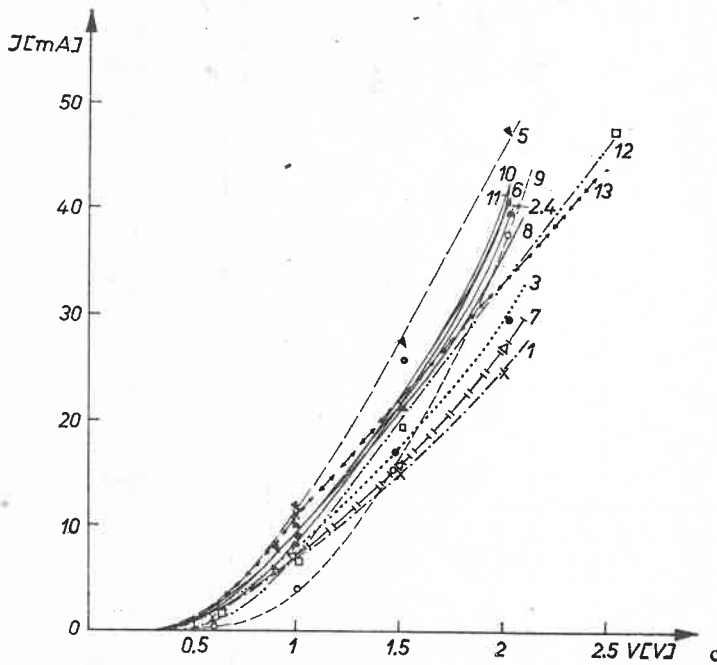
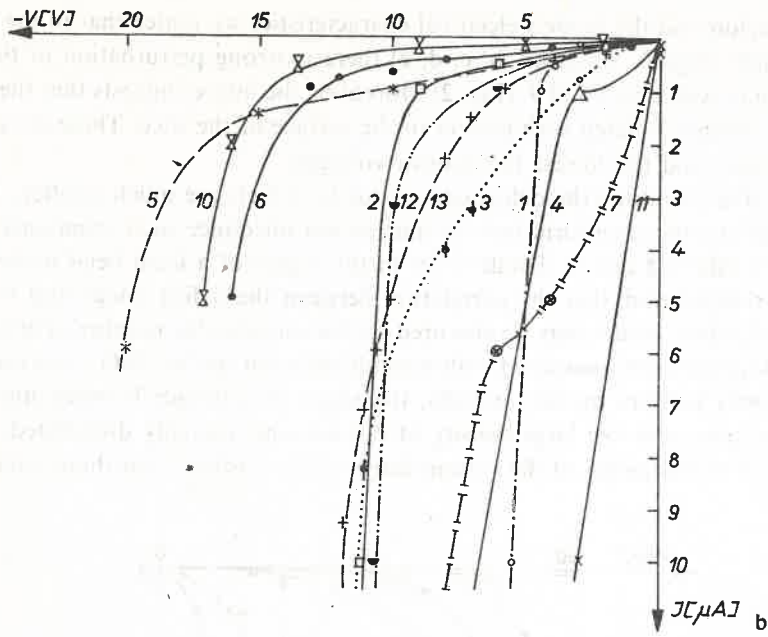


Fig. 8a, b, c. Voltage-current characteristics of the diodes of sample 360B/1. The numerals denote the diodes marked out in Figs 2 and 3. Fig. 8a, b, reverse current characteristics
 Fig. 8c. Forward current characteristics

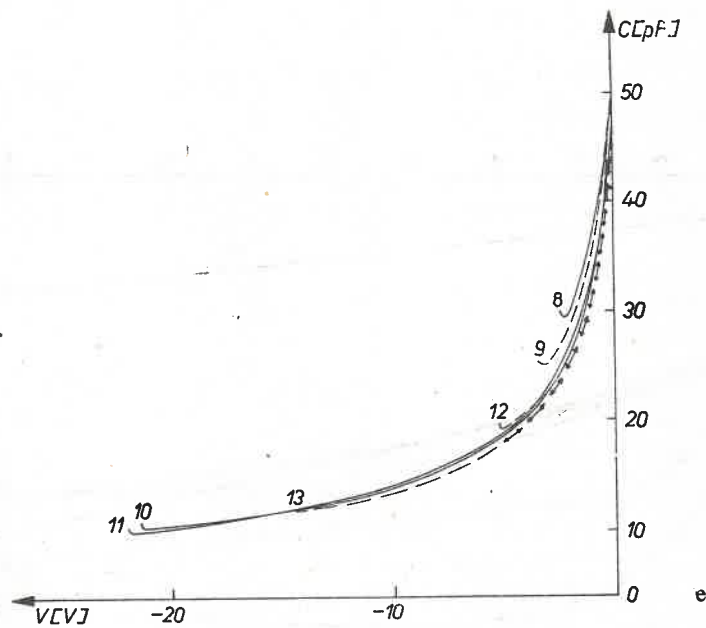
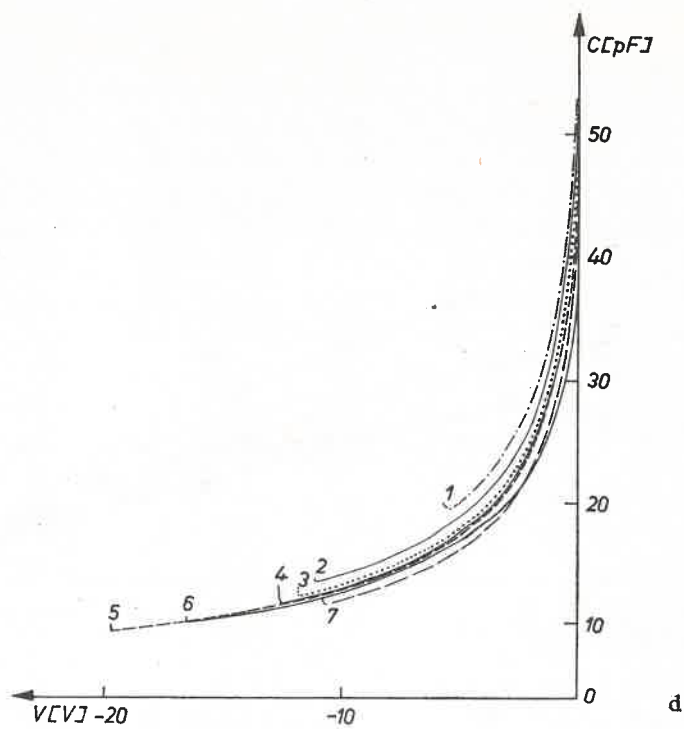


Fig. 8d, e. Voltage-capacitance characteristics of the diodes of sample 360B/1. The numerals denote the diodes marked out in Figs 2 and 3. The C^{-2} vs V relationship is evidence of the abruptness of the $p-n$ junction

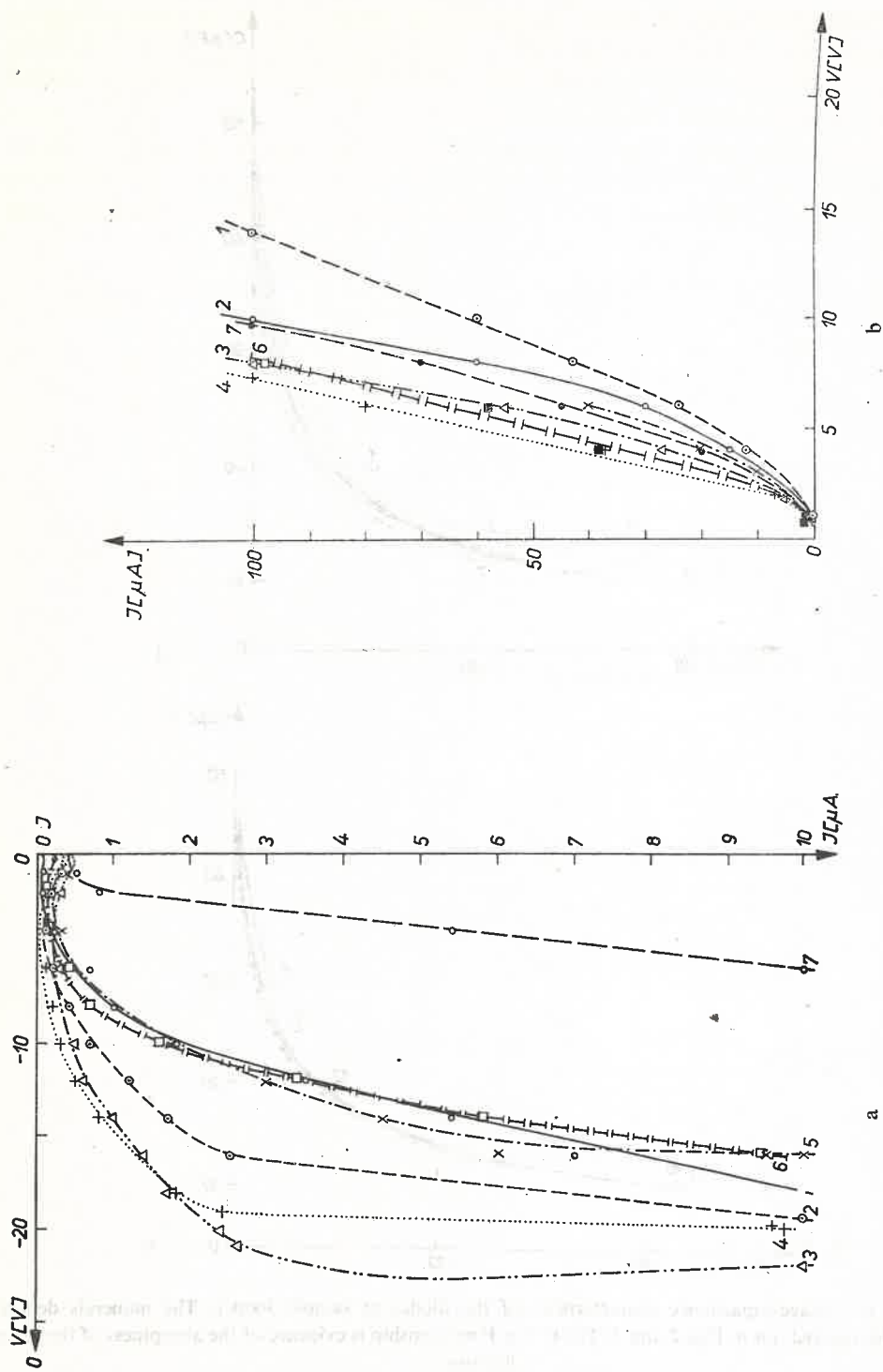


Fig. 9a, b. Voltage-current characteristics of the diodes of sample 360B/4. The numerals denote the diodes marked out in Figs 4a and b. Fig. 9a. Reverse current characteristics. Fig. 9b. Forward current characteristics

In our case the effect of defects on electrical properties may be further concealed by the surface layers existing between the silicon surface and the Al contact deposited at too low temperature. This renders correlation difficult and requires the development of contacts which would eliminate the effect of these layers.

As regards the 360B/4 sample (Figs 4a, b 9a, b, c and Table I), diode 7 exhibits the largest leakage current and lowest breakdown voltage. Its X-ray image reveals strong deformation in the window region. This deformation may be interpreted as a disturbance field

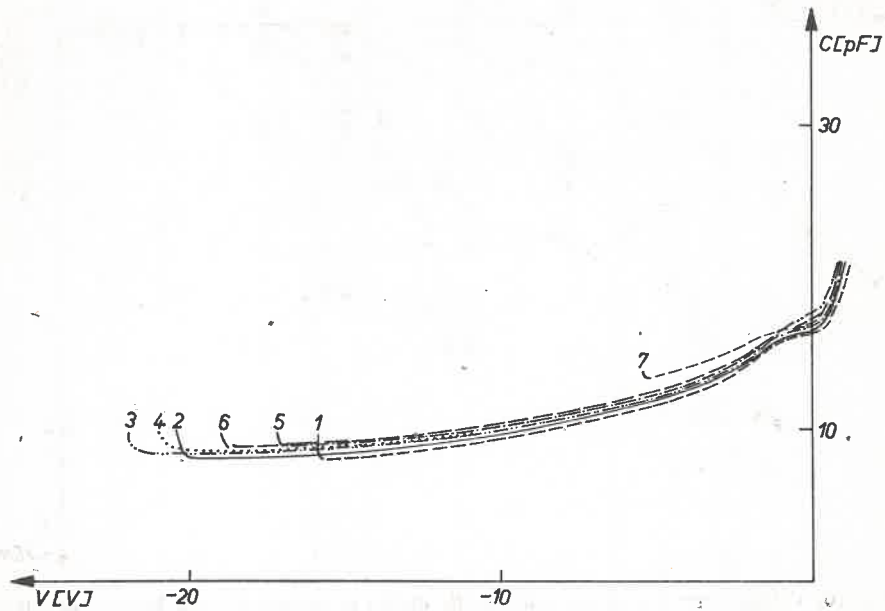


Fig. 9c. Voltage-capacitance characteristics of the diodes of sample 360B/4. The numerals denote the diodes marked out in Figs 4a and b. C^{-2} vs V relationship is evidence that the distribution of impurities at the $p-n$ junctions is linear; this was caused by the diffusion of impurities from the implanted layer during heating of the sample at 800°C

TABLE I

Current flowing through diodes of 360B/4 sample at reverse voltage of 3 and 5 volts

Diode No	Current [μA] at:	
	$V = 3 \text{ V}$	$V = 5 \text{ V}$
1	0.15	0.15
2	0.15	0.3
3	0.25	0.25
4	0.05	0.05
5	0.25	0.4
6	0.15	0.3
7	3.7	7.8

It allows not only the interior of the sample to be examined, but also its surface, once the sample is positioned at the spectrometer axis.

The performed study suggests that there is a correlation between defects causing large deformation, revealed by X-ray methods, and the electrical properties of the diodes. To establish it exactly, however, would require determination of a number of effects, (influence of nonohmicity of contacts, and interface layers between crystal and contacts, the homogeneity of implantation and the shape of interface between implanted and unimplanted area), high statistics and a precise determination of the type of defects.

It was noticed that with increasing dislocation density the diode characteristics become worse (low breakdown voltages, large leakage currents), while the effect of the individual defects is not as distinct.

The authors wish to thank Professor W. Rosiński for showing interest in the results of this study and a discussion of them, Dr K. Sączuk for suggesting the study and with E. Maydell-Ondrusz, M. Sc., for accomplishing the implantation, Dr S. Mączyński, D. Lis, M. Sc., and eng. W. Jung for use of the apparatus and aid in the voltage-current and voltage-capacitance characteristics measurements. Thanks are also due to Dr A. Ambroziak, K. Brochocki, M. Sc., A. Żukowski, M. Sc., and S. Krawczyński for carrying out oxidation, photolithography and contact deposition on the samples, and to K. Godwod, M. Sc., and B. Kunicka for help in our work.

REFERENCES

- Auleytner, J., *Acta Phys. Polon.*, **16**, 35 (1957).
Auleytner, J., *Acta Phys. Polon.*, **A39**, 379 (1971).
Gri, N. I., *Microwave J.*, **14**, 45 (1971).
Howard, J. K., Schwuttke, G. H., *Advances in X-Ray Analysis*, vol. 10, p. 118, Plenum Press-
-New York 1967.
Lang, M., *J. Appl. Phys.*, **29**, 597 (1958).
Serebrinsky, J. H., *Solid-State Electronics*, **13**, 1435 (1970).
Schwuttke, G. H., *Microelectronics and Reliability*, **9**, 397 (1970).
Whelan, M. V., *Solid-State Electronics*, **12**, 963 (1969).